



Role of the intraseasonal IPCO in the absence of typhoons in July 2020

Fei Li¹ · Jianping Li^{1,2} · Hao Wang¹ · Yina Diao¹

Received: 16 July 2022 / Accepted: 27 September 2022 / Published online: 3 October 2022
© The Author(s) 2022

Abstract

The influence of the intraseasonal Indo-western Pacific convection oscillation (IPCO) on the absence of typhoons in July 2020 over the western North Pacific (WNP) was explored. While observation analysis shows that necessary conditions such as sea surface temperature (SST) and vertical wind shear in July 2020 meet the basic requirement of or even are conducive to the formation of typhoon, the unprecedented absence of typhoon over the WNP occurred in July 2020, and it is the first time that no typhoon in July since 1951. Additionally, significant differences were found in the number of typhoons in July between the different phases of the intraseasonal IPCO, and the number in the positive phase of the intraseasonal IPCO was significantly higher than that in the negative phase of the intraseasonal IPCO. In July 2020, the intraseasonal IPCO was in a strong negative phase, with the third lowest index in history and had the strongest inhibition effect on convection over the WNP on record, leading to large-scale circulation anomalies. The strongest descending movement on record inhibited the upward transport of water vapor and the development of cumulus convection, thereby reducing the release of latent heat of condensation and making it difficult to form a typhoon warm-core structure. In addition, the geopotential height increased over the WNP, and the western Pacific subtropical high moved southerly, which inhibited typhoon formation. Simultaneously, the South China Sea monsoon trough weakened significantly, with increased negative vorticity anomaly in the response scale, which hindered disturbance generation. The lowest genesis potential index confirmed that the large-scale circulation anomaly caused by the intraseasonal IPCO had an unprecedented restraining effect on typhoon generation, leading to the absence of typhoons over the WNP in July 2020.

Keywords Tropical cyclone · Absence of typhoon · Intraseasonal Indo-western Pacific convection oscillation · Large-scale circulation condition · Genesis potential index

1 Introduction

The western North Pacific (WNP) is one of the main sources of TCs, producing approximately 36% of TCs (Zhu et al. 2007). TCs with center sustained maximum wind speed exceeding the tropical storm intensity (17.2 m s^{-1} or 34 knots) over the WNP are called typhoons (Zhu et al. 2007;

Li et al. 2016a). Typhoons, especially super typhoons, have huge social and economic impacts in the WNP (Li et al. 2016a; Pandey and Liou 2020). On the one hand, TCs are accompanied by strong winds and torrential rain, bringing serious disasters to the affected areas. According to the statistics, typhoons cause approximately 453 fatalities in the coastal areas of China annually, resulting in a direct economic loss of more than 26 billion yuan (Niu et al. 2011). Typhoon Haiyan in November 2013 killed nearly 6,300 people and caused over \$2.2 billion in economic damage in the Philippines (Pandey and Liou 2020). However, on the other hand, TCs are also a valuable potential resource that bring abundant fresh water to mankind in the WNP. In South and Southeast Asia, the precipitation brought by typhoons accounts for most or even all of the local annual rainfall (Elsberry and Tsai 2016). In addition, TCs also play an important role in driving ocean thermohaline circulation, affecting regional and global climate change (Emanuel 2001;

✉ Jianping Li
ljp@ouc.edu.cn

✉ Yina Diao
diaoyn@ouc.edu.cn

¹ Frontiers Science Center for Deep Ocean Multispheres and Earth System-Key Laboratory of Physical Oceanography-Academy of the Future Ocean, Ocean University of China, Qingdao 266100, China

² Laboratory for Ocean Dynamics and Climate, Pilot Qingdao National Laboratory for Marine Science and Technology, Qingdao 266237, China

Done et al. 2009). Therefore, TC is one of the focuses of weather and climate research in the WNP, and both too many and too few typhoons have important research significance. Every year from July to September (JAS) is the active period of typhoons over the WNP, and it is one of the seasons that typhoons have the greatest impact on the WNP region. Studies have also shown an increasing trend in the number of typhoons and super typhoons in JAS over the WNP in the recent decades (Pandey et al. 2021, 2022). In addition, July is the beginning of the peak season for typhoons, and has approximately four TCs over the WNP every year. However, there was no typhoon generating over the WNP in July 2020, and it is the first time that no typhoon in July since 1951 (Fig. 1). At the same time as the absence of typhoons over the WNP, heavy rains occurred frequently in the Yangtze River basin of China in July 2020. Historically, in July 1954 and 1998, the typhoon activity over the WNP was also at a low tide (only one typhoon), and the rainstorm and flood in the Yangtze River basin were also very serious, which may be related to the intensity and position of western Pacific subtropical high (WPSH) (Zhu et al. 2007; Li et al. 2013b; Qi 2021). Therefore, it is very important to study the causes of the absence of typhoons over WNP in July 2020.

The four well-known necessary conditions for the formation of typhoons are: warm and broad ocean surface (sea surface temperature above 26.5 °C), initial disturbance at low level, sufficient Coriolis force, and weak vertical wind shear (Palmén 1948; Riehl 1948; Gray 1968; Chen and Ding 1979; Wang et al. 2007; Zhu et al. 2007). The results in Sect. 3 of this study show that these four necessary conditions meet the requirements of typhoon generation, suggesting that there may be other complex and special drivers behind the absence of typhoons in July 2020. Wang et al. (2021) used the dynamic genesis potential index to show the impacts of large-scale circulation conditions on typhoon genesis, and their numerical experiments showed that warming of the Indian Ocean could trigger abnormal anticyclone over the WNP, leading to the absence of typhoons.

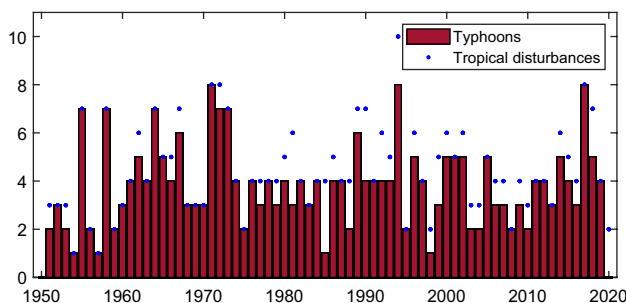


Fig. 1 Time series of typhoons (bar) and tropical disturbances (dot) over the WNP in July from 1979 to 2020

Convection also plays an important role in TC formation. Previous studies on the convective characteristics over the tropical Indo-western Pacific using outgoing longwave radiation (OLR) data showed an out-of-phase relationship in convection variation between the Indian Ocean and the WNP, and the location and phase of convection activities varied in different seasons (Lau and Chan 1985, 1986; Zhu and Wang 1993; Lee et al. 2012). Li et al. (2013b) found that this convective dipole phenomenon also has important signals on interannual timescales, but the centers of convective actions remain largely the same and define the out-of-phase convection anomalies over the Indo-western Pacific as the Indo-western Pacific convection oscillation (IPCO). Zhang et al. (2015) found that the IPCO has significant intraseasonal variations, and the average locations of the convection centers of the intraseasonal IPCO change slightly and lie over the eastern equatorial Indian Ocean (EEIO) (5°S–10°N, 70°–100°E) and the WNP (5°–20°N, 110°–160°E), respectively. Wang et al. (2018, 2019) explored the modulation effect of the intraseasonal IPCO on TC genesis location, frequency, and path over the Indo-western Pacific. They found that there tend to be more TCs over the WNP when the intraseasonal IPCO was in its positive phase, whereas the TC genesis frequency is lower in its negative phase. In addition, Wang et al. (2018) explored the possible physical mechanism by which the intraseasonal IPCO affects large-scale circulation and its impact on typhoon generation. In July 2020, the IPCO turns to its strong negative phase. Does the intraseasonal IPCO play an important role in the absence of typhoon in July 2020? What is the physical mechanism of the intraseasonal IPCO inhibiting typhoon formation? These questions are the motivation for the present study.

The remainder of this paper is organized as follows: Sect. 2 briefly reviews the data and methodologies used in the analyses. Section 3 explores necessary conditions for typhoon genesis over the WNP in July 2020. Sections 4 and 5 show the influence of the intraseasonal IPCO on typhoon genesis and circulation and the absence of typhoons in July 2020, respectively. Section 6 presents a summary of the key results and discussion.

2 Data and methodology

2.1 Data

Daily datasets analyzed from 1979 to 2020, consisted of reanalysis data (Kalnay et al. 1996) and interpolated OLR data (Liebmann and Smith 1996) from the National Centers for Environment Prediction (NCEP)–National Centers for Atmospheric Research (NCAR), including geopotential height, relative humidity, vertical velocity, sea surface

temperature, wind field, and interpolated OLR, with a horizontal spatial resolution of 2.5° .

The best-track data for TC activity over the WNP during 1951–2020 were obtained from the Regional Specialized Meteorological Center (RSMC) of the Japan Meteorological Agency (JMA). Only TCs that reached tropical storm intensity (maximum sustained 10 m wind speed $\geq 17.2 \text{ m s}^{-1}$ or 34 knots) were used in our analysis.

2.2 Statistical methods

To study the influence of the intraseasonal IPCO, anomalies of the aforementioned meteorological elements, except for typhoon data and sea surface temperature, were applied to a 30–60-day Lanczos bandpass filter using 305 weights, and the response function is shown in Fig. 2. It can be seen that the signals beyond 30–60 days are basically removed.

Based on previous study (Li et al. 2013a; Zhang et al. 2015), the intraseasonal IPCO index has been defined as

$$\text{IPCOI} = \text{OLR}_{\text{EEIO}} - \text{OLR}_{\text{WNP}}, \quad (1)$$

where OLR_{EEIO} and OLR_{WNP} are the normalized areal-averaged time series of the OLR anomalies over the EEIO (5°S – 10°N , 70° – 100°E) and WNP (5° – 20°N , 110° – 160°E), respectively. According to the value of IPCO index (IPCOI), the intraseasonal IPCO can be divided into three phases: positive ($\text{IPCOI} > 1$), negative ($\text{IPCOI} < -1$), and neutral ($-1 < \text{IPCOI} < 1$).

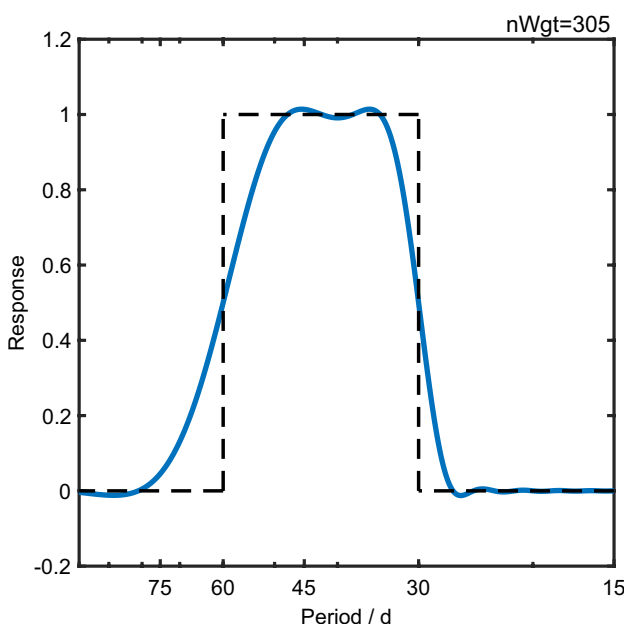


Fig. 2 The response function of the 30–60-day Lanczos bandpass filter. The filter has 305 weights and cutoff periods of 30 and 60 days

Since the data used in this paper are daily data and have been filtered by a 30–60-day Lanczos bandpass filter, the data have a large autocorrelation. The statistical significance of the correlation between two autocorrelated time series is assessed via the two-tailed Student's *t*-test using the effective number of degrees of freedom (N^{eff}) provided by the following approximation (Pyper and Peterman 1998; Li et al. 2012a, b; Li et al. 2013a; Xie et al. 2014; Sun et al. 2015):

$$\frac{1}{N^{\text{eff}}} \approx \frac{1}{N} + \frac{2}{N} \sum_{j=1}^N \frac{N-j}{N} \rho_{XX}(j) \rho_{YY}(j), \quad (2)$$

where N is the sample size, and $\rho_{XX}(j)$ and $\rho_{YY}(j)$ are the autocorrelations of the two sampled time series X and Y at time lag j , respectively.

Composite and correlation analyses are performed to explore the possible physical mechanisms.

2.3 Genesis potential index

To further confirm our results, 30–60-day Lanczos bandpass-filtered genesis potential index (GPI) anomalies are employed in this study. Developed by Emanuel and Nolan (2004), GPI has been widely used to diagnose interannual and intraseasonal variabilities for TC genesis, and examine the impacts of large-scale circulation anomalies on TC genesis (Camargo et al. 2007, 2009; Jiang et al. 2012; Zhao et al. 2015a, b; Wang et al. 2018). The GPI is defined as

$$\text{GPI} = (1 + 0.1V_{\text{shear}})^{-2.0} \left(\frac{rh_{\text{um}}}{50} \right)^{3.0} \left(\frac{PI}{70} \right)^{3.0} \left| 10^5 \zeta_a \right|, \quad (3)$$

where V_{shear} is the magnitude of the vertical wind shear between 850 and 200 hPa (m s^{-1}), rh_{um} is the relative humidity (%) at 600 hPa, PI is the potential intensity (m s^{-1}) and ζ_a is the absolute vorticity (s^{-1}) at 850 hPa. The definition of PI is defined by Bister and Emanuel (1998), based on Emanuel (1995):

$$MPI^2 = \frac{C_k}{C_D} \frac{T_s - T_o}{T_o} (h_o^* - h^*), \quad (4)$$

where C_k and C_D denote the surface enthalpy and momentum exchange coefficients, respectively, T_s and T_o are the sea surface temperature and outflow temperature, respectively, h_o^* is the saturation moist static energy of the sea surface, and h^* is the saturated moist static energy of the free atmosphere.

3 Necessary conditions for typhoon genesis over the WNP in July 2020

The seasonal variation of tropical cyclones is related to the difference of environmental condition in which they are generated, and this difference mainly refers to the difference of large-scale climatic background field (Chen and Ding 1979). Palmén (1948) and Riehl (1948) successively put forward five basic conditions for typhoon generation. Gray (1968) proposed six necessary conditions for the generation of tropical cyclones based on the prediction experience of the National Hurricane Center. Among these views, there are four necessary conditions that are unanimously agreed upon (Chen and Ding 1979). These conditions are: warm sea surface; The vertical wind shear of troposphere is smaller; Initial disturbance at the low-level; The generation location is outside the five latitudes of the equator (Chen and Ding 1979; Zhu et al. 2007). Therefore, before investigating the possible impact of the intraseasonal IPO on typhoons, the above four necessary conditions of typhoon genesis are explored to confirm whether the absence of typhoon genesis is caused by the failure of meeting the basic requirement of these conditions.

The sea surface temperature (SST) is the fundamental thermal condition and should be greater than 26.5 °C for typhoon generation (Zhu et al. 2007). The warm sea surface is the basis of the formation of a warm-core structure, since it contains a large amount of heat, and strong evaporation. Through the turbulence transport between the air and sea, a large amount of warm and wet air is obtained from the lower atmosphere where the disturbance is located, making the atmospheric stratification conditionally unstable (Zhu et al. 2007). Figures 3a and 4a show the spatial patterns of SST anomalies over the WNP in July 2020 and the time series of the area-averaged SST from 1979 to 2020, respectively. It is seen that the areal-averaged SST over the WNP in July 2020 is abnormally high exceeding 30 °C, the highest since 1979. In addition, Fig. 3c shows the generation location of typhoons and tropical disturbances in July from 1979 to 2020, which are basically generated between 5°N and 25°N. It is clear that the SST over the WNP in July 2020 is abnormally warm, providing abundant water vapor and heat supply, conducive to the formation and development of typhoons.

In addition to warm SST, weak vertical wind shear is also crucial for the formation of typhoon (Goldenberg and Shapiro 1996; Bessafi and Wheeler 2006). When the vertical wind shear is small, the condensation latent heat produced by the cumulus is concentrated in a limited space, favoring formation of the warm-core structure of the typhoon (Zhu et al. 2007). In contrast, the latent heat of condensation will be rapidly transported from the initial

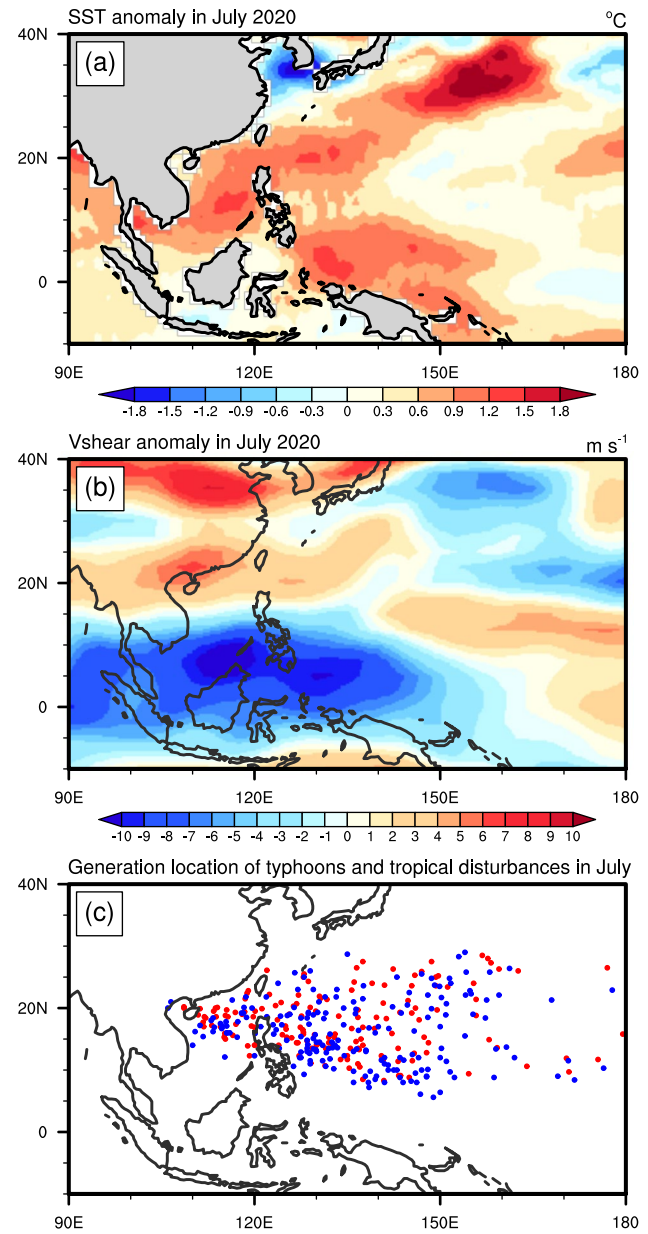


Fig. 3 Spatial patterns of **a** SST anomaly (°C) and **b** vertical wind shear anomaly ($m s^{-1}$) over the WNP in July 2020 **c** Location of typhoon and disturbance generation. The blue dots indicate the location of tropical disturbances, and the red dots indicate the location of typhoons

disturbance if the vertical wind shear is extremely large, and a large area becomes slightly warm with low pressure, which is unfavorable for the formation of typhoon (Zhu et al. 2007). Figures 3b and 4b show the spatial patterns of the vertical wind shear anomaly over the WNP in July 2020 and the time series of the areal-averaged vertical wind shear from 1979 to 2020, respectively. In terms of spatial distribution (Fig. 3b), the vertical wind shear south of 15°N is obviously smaller than the climatological

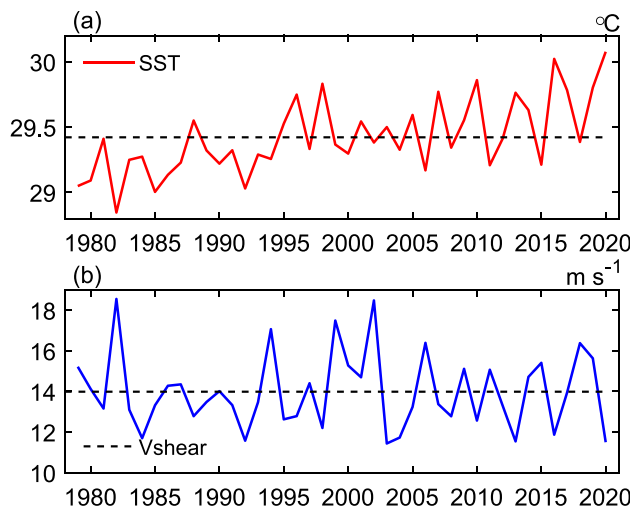


Fig. 4 Time series of areal-averaged **a** SST ($^{\circ}\text{C}$) and **b** vertical wind shear (m s^{-1}) over the WNP (5°N – 25°N , 110°E – 160°E) from 1979 to 2020. Dashed lines indicate the climatological normal

Table 1 Number of tropical disturbances in July 2020 and climatological normal over the WNP

	Climatological normal	2020
Tropical disturbances	4.6	2

normal, and the wind shear north of 15°N is slightly larger. The areal-averaged results (Fig. 4b) show that the vertical wind shear in July 2020 is generally lower than the climatological normal, which means that the condensation latent heat is easier to maintain in a small area and is thus favorable to the formation of the warm-core structure of typhoons.

Besides, a low-level disturbance is needed at the initial time, as tropical disturbances can release the unstable energy of the unstable atmosphere and transform it into the kinetic energy of TC development (Riehl 1948; Zhu et al. 2007). The number of tropical disturbances is listed in Table 1. In July 2020, two tropical disturbances occurred over the WNP, less than half the climatological normal. Despite such favorable SST and vertical wind shear conditions, the two tropical disturbances did not develop into typhoons. Thus, other factors must have played a strong role in the process of tropical disturbance and its development into typhoons. As mentioned above, the intraseasonal IPCO could modulate the generation and movement of TCs by influencing the steering flow, energy conversion, and energy propagation during the boreal extended summer (May–October) (Wang et al. 2018, 2019). The following sections explore the possible influence of the intraseasonal IPCO on the genesis of typhoons.

Table 2 The composite number of typhoons over the WNP in July during the positive and negative intraseasonal IPCO phases (1979–2020) and their difference

	IPCO (+)	IPCO (-)	Difference (IPCO (+)–IPCO (-))
Typhoons	4.8	2.8	2.0*

*Indicates significance at the 95% confidence level using the Student's *t* test

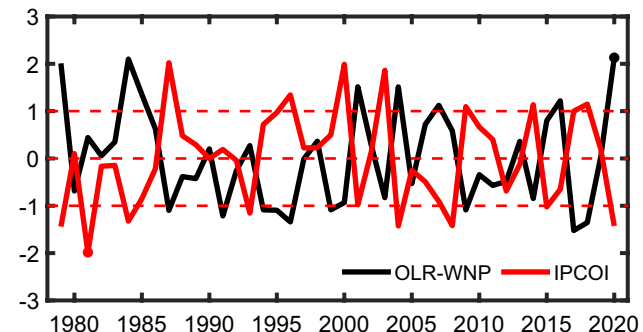


Fig. 5 Time series of IPCOI and areal-averaged OLR over the WNP (5°N – 20°N , 110°E – 160°E) in July from 1979 to 2020. Dots indicate the variables in those years that had minimum or maximum values over the study period

4 Influence of the intraseasonal IPCO on the genesis of typhoons and large-scale circulation anomalies

The frequency of typhoon genesis over the WNP changed during the different phases of the intraseasonal IPCO in July. Table 2 shows the composite number of typhoons over the WNP in July during the positive and negative intraseasonal IPCO phases from 1979 to 2020 and their differences. There are significant differences in number of typhoons generated in July in the different intraseasonal IPCO phases, and tends to be more typhoons over the WNP during the positive phase of the intraseasonal IPCO (about 1.7 times more than in the negative phases), consistent with the results reported by Wang et al. (2018) on boreal extended summer (May–October). The IPCOI could measure the difference in convective intensity between the EEIO and WNP characterizing the phase and strength of the intraseasonal IPCO. In the positive phase of the intraseasonal IPCO, convection over the WNP is strengthened and that over the EEIO is inhibited, while in the negative phase of the intraseasonal IPCO, convection over the WNP is weakened and that over the EEIO is strengthened. Figure 5 shows the time series of IPCOI and area-averaged OLR over the WNP (5 – 20°N , 110 – 160°E) in July from 1979 to 2020. As can be seen, the intraseasonal IPCO in

July 2020 is the one of the strongest negative phases in history, and further indicated by the area-averaged band-passed filtered OLR over the WNP was also experiencing the weakest convective intensity on record, which may be closely related to the absence of typhoon.

Previous studies have found that the IPCO could provide a background field for convective strengthening (weakening) over the WNP and EEIO, and further affect local circulation changes. For example, in the positive phase of IPCO in summer, when the WNP convection is strengthened, the low-level convergence is strengthened, the monsoon in Southeast Asia is strengthened, and Southeast Asia becomes cooler (Zheng et al. 2017). Wang et al. (2018) found that in the positive intraseasonal IPCO phase, when the convection over the WNP is enhanced, the low-level convergence and middle-level ascending motion are enhanced, the

relative humidity in the middle level increases, and there is an abnormal cyclonic over the WNP, and ridge of the WPSH at 850 hPa will move northward. The opposite situation holds for the negative phase. These findings suggest that the IPCO could influence the generation of typhoons over the WNP by affecting local circulation factors. In July 2020, the intraseasonal IPCO had an unprecedented strong inhibition on convection over the WNP, which may have inhibited the generation and development of typhoons by influencing large-scale circulation anomalies. This was followed by further investigation on the circulation anomalies in July during the different phases of the intraseasonal IPCO.

The anomalies of large-scale circulation affected by the intraseasonal IPCO could be characterized by the 30–60-day Lanczos bandpass-filtered data. Figure 6 shows the composite difference of the 200 hPa and 850 hPa divergence,

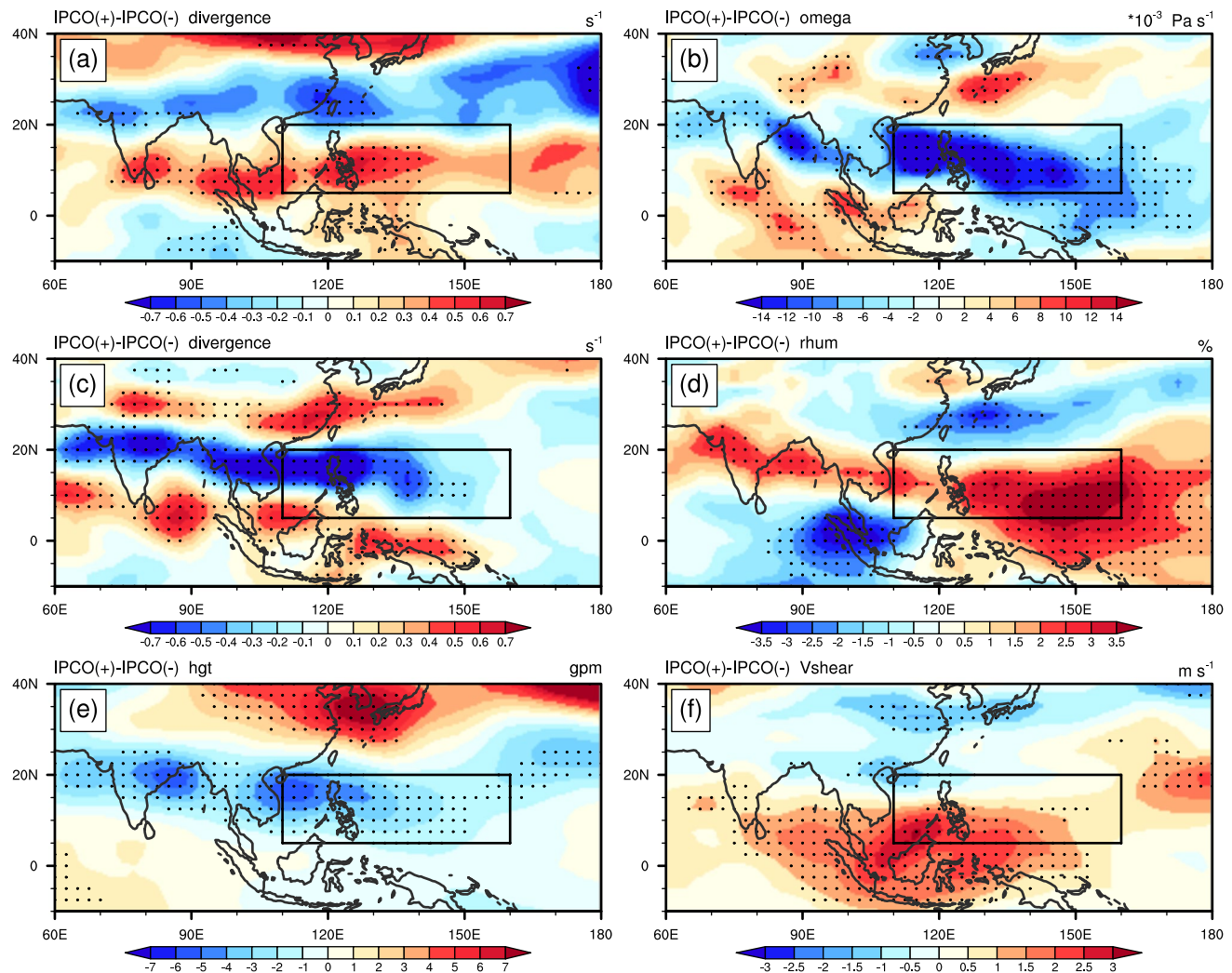


Fig. 6 Composite difference in **a** 200 hPa divergence (s^{-1}), **b** 500 hPa vertical velocity ($Pa\ s^{-1}$), **c** 850 hPa divergence (s^{-1}), **d** 600 hPa relative humidity anomalies (%), **e** 500 hPa geopotential height anomalies (gpm), and **f** vertical wind shear ($m\ s^{-1}$) between the positive and

negative intraseasonal IPCO phases in July for the period 1979–2020. The stippled regions denote significance at the 99% confidence level using the Student's *t* test. The black rectangle denotes the key areas of the intraseasonal IPCO over the WNP (5° – 20° N, 110° – 160° E)

500 hPa vertical velocity and geopotential height, 600 hPa relative humidity anomalies, and vertical wind shear in July between the positive and negative IPOC phases. Significant differences are observed in large-scale circulation under different the intraseasonal IPOC phases, and the large-scale circulation anomalies present in the north–south dipole distribution.

In the positive phase of the intraseasonal IPOC, the upper-level divergence, low-level convergence, and middle-level ascending motion are enhanced in the range of 5°N–20°N when the large-scale convection over the WNP is strengthened. Such large-scale circulation anomalies are favorable to the lifting and development of low-level disturbances, and can also enhance the upward movement of water vapor and the development of local cumulus convection. Previous studies have shown that the relative humidity of the middle atmosphere is closely related to the formation of typhoons, and typhoons over the WNP only form in areas where the seasonal mean of the relative humidity of the middle troposphere is high (Chen and Ding 1979; Zhu et al. 2007). Higher relative humidity is conducive to the development of cumulus convection. Generally, the buoyancy of cumulus clouds will be reduced due to the inhalation of drier air around them. However, in the humid surroundings, the buoyancy of clouds will not be significantly reduced, which can promote the development of cumulus clouds and the release of condensation latent heat (Chen and Ding 1979; Zhu et al. 2007). In addition, the strongest convective activity occurs in the middle atmosphere, hence the relative humidity in the middle atmosphere represents the available latent heat of condensation to some extent (Gray 1979; Wang and Moon 2017; Wang et al. 2018). Figure 6d illustrates the composite difference between the positive and negative phases of the relative humidity anomalies at the 600-hPa level. Owing to the strengthening of convection and upward water vapor transport, in the intraseasonal IPOC positive phase, the relative humidity in the middle troposphere increases and cumulus convection releases more latent heat of condensation, contributing to the development of the warm-core structure of the typhoon. The opposite situation holds for the negative phase.

The WPSH is an important circulation system in the WNP. Studies have shown that it has an important influence on the typhoon activity over the WNP (Lu 2001; Li et al. 2011). Most typhoons over the WNP occur on the southern side of the WPSH (Zhu et al. 2007). When the west ridge point of WPSH is eastward and the ridge position is northward, the typhoon activity is strengthened (Ho et al. 2004; Zhu et al. 2007; Zheng et al. 2013). In the positive phase of the intraseasonal IPOC, owing to the strengthening of convection (south of 25°N), troposphere heating is dominated by condensation latent heat release. According to the potential tendency equation, as nonadiabatic heating

increases with height, the geopotential height decreases (Zhu et al. 2007). As shown in Fig. 6e, the low-value center of the geopotential height is located in the South China Sea, whereas the high-value center is in the Sea of Japan during the positive phase of the intraseasonal IPOC, which is favorable to the northward uplift of the WPSH and the development of tropical disturbance over the WNP. When the intraseasonal IPOC is in a negative phase, the WPSH is abnormally intensified and the ridge position is southward, which suppresses TC genesis over the WNP.

The formation of typhoons requires tropical disturbances as embryos; hence the number of tropical disturbances restricts the number of typhoons to some extent (Chen and Ding 1979; Zhu et al. 2007). Moreover, tropical disturbance is the embryonic state of TC, which can convert the unstable energy of an unstable atmosphere into kinetic energy of TC development (Zhu et al. 2007). The intertropical convergence zone (the South China Sea monsoon trough in the WNP) is the main area of tropical disturbance generation (Ritchie and Holland 1999; Li et al. 2016b), and about 80–85% of the tropical disturbances over the WNP are derived from the South China Sea monsoon trough (SCSMT) and about 10% are derived from the easterly wave, which is mainly affected by the position of the WPSH (Zhu et al. 2007; Zhang and Zhang 2011). Figure 7 shows the composite of the vorticity anomalies and monthly mean horizontal wind at the 850-hPa level. The position and intensity of the South China Sea monsoon trough (SCSMT) are significantly different in the different phases of the intraseasonal IPOC. In the positive phase of the intraseasonal IPOC, the SCSMT is much stronger than that in the negative phase, and the trough line can reach 150°E. In addition, the north–south range of the SCSMT covers the main area of typhoon generation, and water vapor and heat abound in the SCSMT. The airflow easily converges and then rises in this area, which is conducive to the generation and uplifting of tropical disturbances. The positive anomaly of the vorticity at the trough line leads to a decrease in the Rossby deformation radius, which reduces the scale of response and increases the conversion of latent heat release to rotational motion, thus facilitating the generation of tropical disturbances (Hack and Schubert 1986). In the year of the negative phase of the intraseasonal IPOC, the intensity of the SCSMT is obviously weaker, and the vorticity is a significantly negative anomaly, unfavorable for the generation and development of tropical disturbances.

In addition, Fig. 6f shows that the distribution of the vertical wind shear anomaly dipole is 5 latitudes south of the other atmospheric circulation anomalies as a whole, with the high-value center located in the south of the South China Sea (10°S–15°N, 80°–160°E). In the positive phase of the intraseasonal IPOC, the vertical wind shear is abnormally high south of 15°N, which is not favorable for the maintenance of condensation latent heat and the formation of a

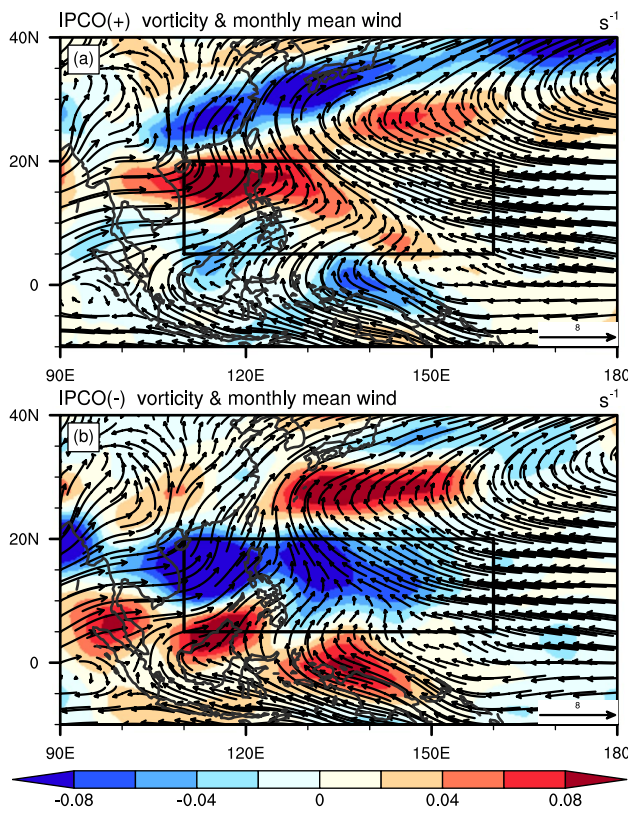


Fig. 7 **a** Composite map of the 850 hPa monthly mean horizontal wind (vector, m s^{-1}) and vorticity anomaly (shaded, s^{-1}) over the WNP in July for the period 1979–2020 for the positive intraseasonal IPOC phase. **b** As in (a), but for the negative intraseasonal IPOC phase. The black rectangle indicates the same as in Fig. 6

typhoon warm heart structure, whereas it is the opposite north of 15°N . In general, IPOC can modulate the generation of typhoons by influencing environmental factors such as vorticity, vertical velocity, relative humidity, WPSH and SCSMT. Except for vertical wind shear, circulation anomalies have similar effects on typhoons formation.

To further verify the effect of IPOC on typhoon, we used GPI. To further verify the influence of IPOC on typhoon activity, the GPI is employed. Previous research has shown that the GPI replicates the interannual variations of TC genesis in several different basins on intraseasonal timescales and reflects the influence of large-scale circulation conditions on TC genesis (Camargo et al. 2007, 2009; Jiang et al. 2012; Zhao et al. 2015a, b). The GPI is mainly influenced by four factors: low-level vorticity, middle-level relative humidity, vertical wind shear, and potential intensity. Table 3 shows the correlation coefficients between IPOCI and GPI and its four elements, and IPOCI is highly correlated with both, indicating that GPI can be used to characterize the influence of environmental conditions caused by the IPOC on typhoon generation, in accordance with a previous study (Wang et al. 2018).

Table 3 Correlation coefficient between IPOCI and areal-average vertical wind shear (Vshear), 600 hPa relative humidity (Rhum), potential intensity (PI), 850 hPa absolute vorticity, and GPI over the WNP in July

	Vshear	Rhum	PI	Vorticity	GPI
Correlation coefficient	0.72*	0.77*	-0.42*	0.78*	0.58*

*Indicates significance at the 99% confidence level using the Student's *t* test

Figure 8 shows the composite difference between the positive and negative IPOC phases in the GPI in July. In the key area of the WNP part of the intraseasonal IPOC, positive values indicate that more typhoons tend to be generated in the intraseasonal IPOC-positive phase than in the negative phase.

5 Role of the intraseasonal IPOC in the absence of typhoon in July 2020

As mentioned above, IPOC can modulate the generation of typhoons by influencing large-scale environmental factors over the WNP in the different phases of intraseasonal IPOC. Compared with the positive phase, the circulation anomalies in the negative phase of the intraseasonal IPOC were unfavorable for the generation of TCs over the WNP. In addition, the intraseasonal IPOC in July 2020 is a strong negative phase, and the inhibition on convection over its WNP is unprecedentedly strong. To explain the role of the intraseasonal IPOC in the absence of typhoons over the WNP, three possible influencing pathways are proposed: the influence on cumulus convection, WPSH, and SCSMT.

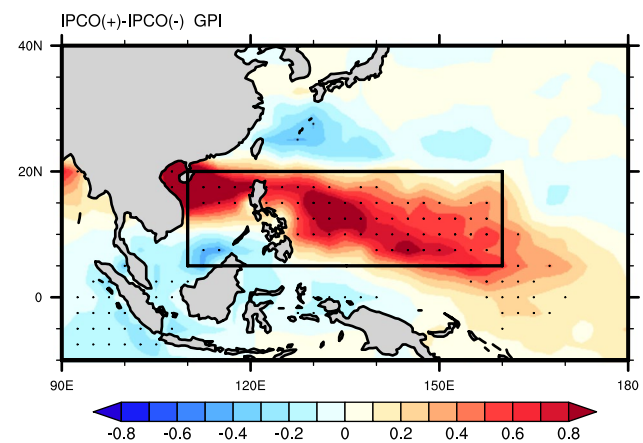


Fig. 8 As in Fig. 6, but for the GPI

5.1 Cumulus convection anomalies

As mentioned above, the condensation latent heat released by cumulus convection is an important energy source for the development of typhoons, and the middle-level relative humidity can characterize the available latent heat of condensation of cumulus convection to some extent. Figures 9 and 10 show the anomalies of the aforementioned large-scale atmospheric circulation in July 2020. Figure 9a shows an anomalous anticyclone in the lower troposphere over the WNP, with its center over the South China Sea and the eastern part of the Philippines, and an abnormal cyclone located along the southeast coast of China. The low-level divergence field corresponds well to the position of the wind field, the divergence is strengthened over the South China Sea and the eastern part of the Philippines, and the convergence is

strengthened along the southeast coast of China, presenting a north–south dipole distribution. The position of the strongest subsidence movement is consistent with the low-level divergence center and the center of the anomalous anticyclone over the WNP (Fig. 9a and b). Such circulations are not conducive to the lifting and development of low-level disturbances over the WNP in July 2020, as the air mass must undergo a considerable amount of forced uplift before reaching the height of free convection and then obtain unstable energy from the atmosphere to continue development. The strengthening of the sinking movement inhibits the upward transport of water vapor, leading to a significant negative anomaly in tropospheric relative humidity (Fig. 10), indicating suppression of cumulus convection and the reduction in the release of latent heat of condensation over the WNP in July 2020. By simplifying the equations of motion, we

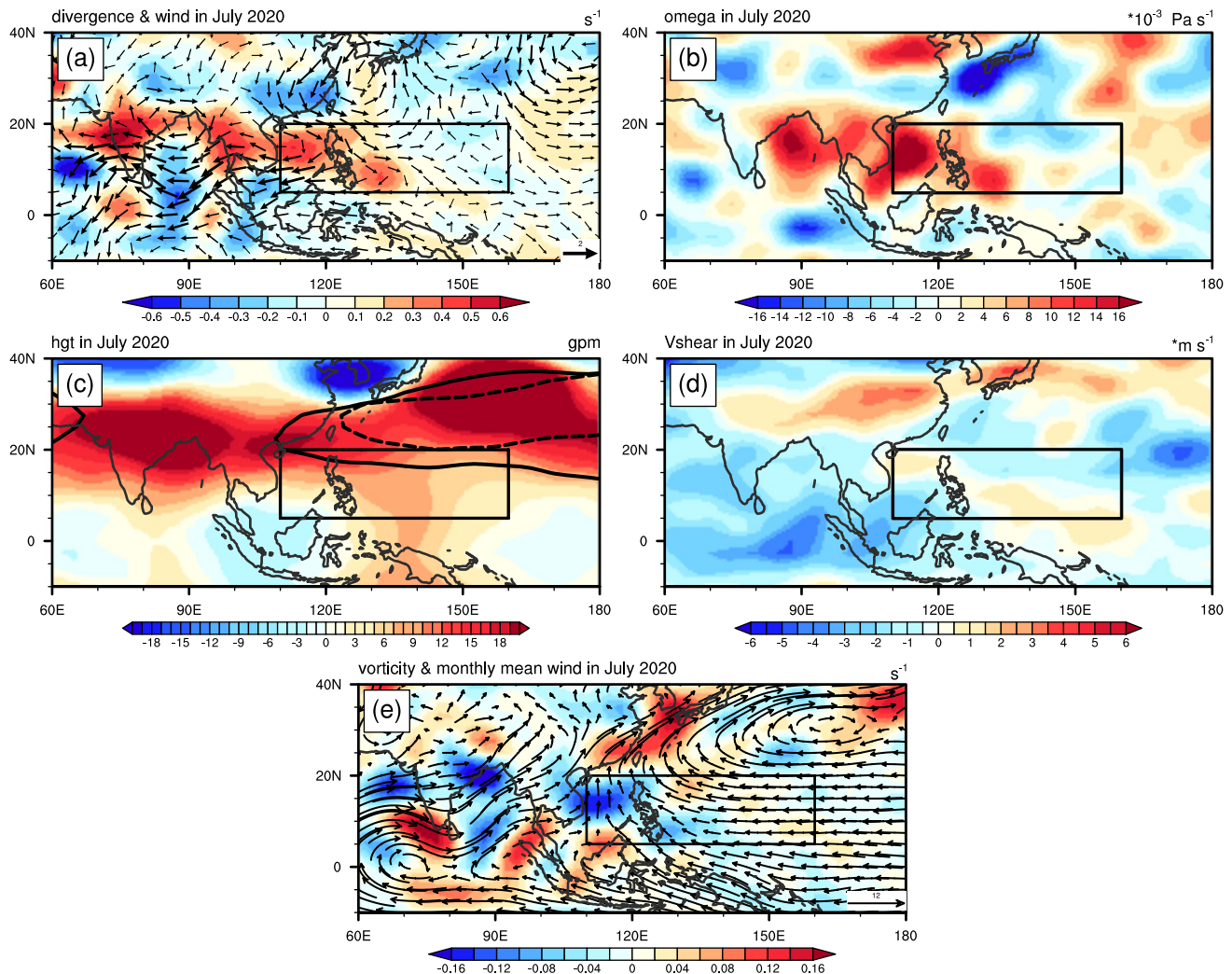


Fig. 9 Anomalies of the **a** 850 hPa divergence (shaded, s^{-1}) and horizontal wind (vector, $m s^{-1}$), **b** 500 hPa vertical velocity (Pa s^{-1}), **c** 500 hPa geopotential height (gpm), and **d** vertical wind shear ($m s^{-1}$) in July 2020. **e** The 850 hPa vorticity anomaly (s^{-1}) and monthly

mean horizontal wind (vector, $m s^{-1}$) over the WNP in July 2020. Thick solid and dashed lines in **(d)** indicate the 5880 gpm isoline of 500 hPa geopotential height in July 2020 and climatological mean, respectively. The black rectangle indicates the same as in Fig. 6

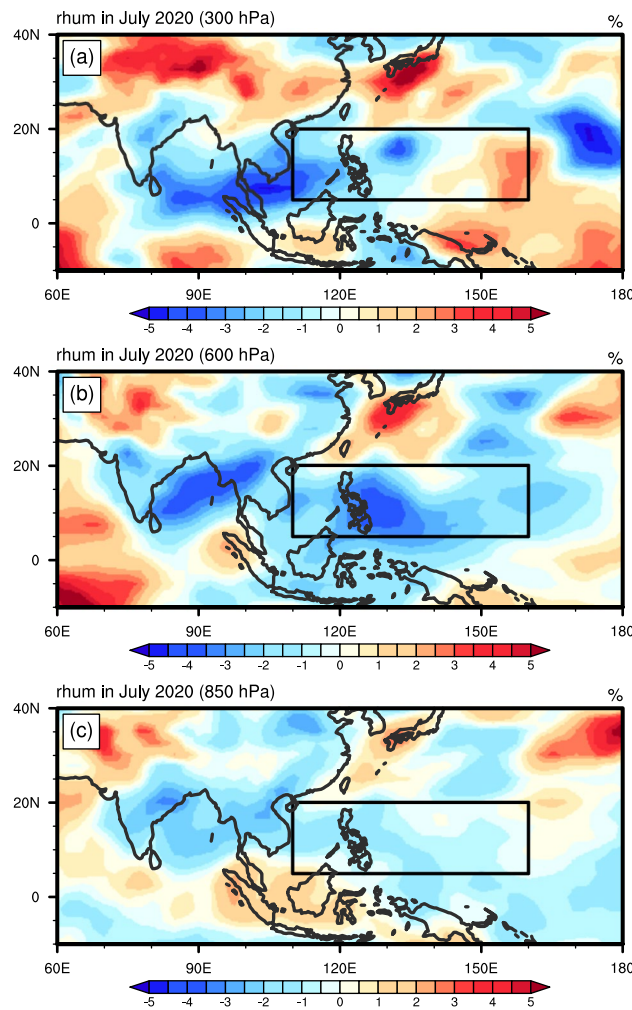


Fig. 10 As in Fig. 9, but for the **a** 300 hPa rhum (%), **b** 600 hPa rhum (%), **c** 850 hPa rhum (%)

obtained the relationship between the radial temperature gradient $\partial T_r / \partial r$ and the vertical tangential wind shear $\partial v / \partial \ln p$ (Anthes 1982; Holland 1987; Zhu et al. 2007; Kepert 2010; Wang et al. 2018):

$$\frac{\partial v}{\partial \ln p} \left(f + \frac{2v}{r} \right) = -R_d \frac{\partial T_v}{\partial r}, \quad (5)$$

where f is the Coriolis parameter, v the tangential velocity ($v > 0$ represents the cyclonic flow), r is radial distance to the center of TC, p is pressure, R_d is the gas constant for dry air, and T_v is virtual temperature. Equation (5) shows that the TC warm-core structure favors weakening of the TC cyclonic circulation with height, which implies that the warm-core structure plays a vital role in the development of TC (Wang et al. 2018). As shown in Fig. 10b, the relative humidity in the middle atmosphere is negative anomaly over the WNP in July 2020, which covers most typhoon-generating areas.

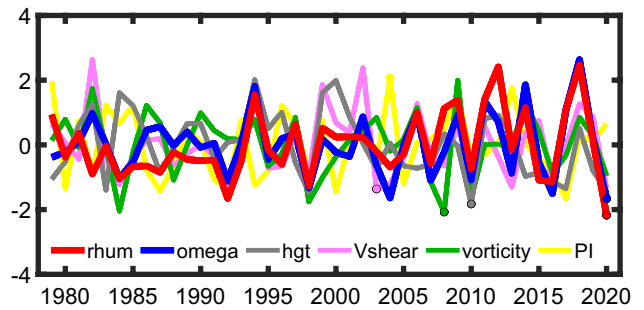


Fig. 11 Time series of areal-averaged 600 hPa relative humidity, 500 hPa vertical velocity and geopotential height, vertical wind shear, 850 hPa absolute vorticity and potential intensity over the WNP (5°N–20°N, 110°E–160°E) in July. The opposite signs of geopotential height and vertical velocity are used here. Dots indicate that the variables in those years had the minimum value over the study period

In addition, the relative humidity in the high-level and low-level troposphere is also negative anomalies, which means that the condensation latent heat released by cumulus convection decreases, the release of condensation latent heat decreases, which is not conducive to the development of typhoon structure over the WNP in July 2020. Figure 11 shows the time series of the areal-average 600 hPa relative humidity, 500 hPa vertical velocity and geopotential height, vertical wind shear, and 850 hPa absolute vorticity over the WNP in July. It can be seen that the vertical velocity and relative humidity in 2020 are the lowest since 1979, indicating that the subsidence movement in July 2020 was the strongest, and the cumulus convection was the weakest, which hindered the development of the typhoon structure. Moreover, about half of the vertical wind shear between 5 and 25°N has a negative anomaly, which makes it harder for the latent heat of condensation to concentrated in a limited space, resulting in difficulty in typhoon formation (Fig. 9d).

5.2 WPSH anomalies

The intensity and position of the WPSH have a great influence on the typhoon activity. The intraseasonal IPOC can influence the position and intensity of the WPSH by influencing the geopotential height. Wang et al. (2018) found that in the positive intraseasonal IPOC phase, when the convection over the WNP is enhanced, the low-level convergence and middle-level ascending motion are enhanced, the relative humidity in the middle level increases, and there is an abnormal cyclonic over the WNP, and the accessory high ridge at 850 hPa will move northward.

In July 2020, in the strong negative intraseasonal IPOC phase, the middle-level sinking motion was enhanced. And owing to the decrease in cumulus convective intensity and condensation latent heat release, tropospheric heating over the WNP is dominated by surface long-wave radiation

heating, which means that nonadiabatic heating increases with decreasing height. According to the potential tendency equation, as nonadiabatic heating decreases with height, the geopotential height increases (Zhu et al. 2007). As shown in Fig. 9c, the geopotential height over the WNP in July 2020 was abnormally high and conducive to the strengthening of the WPSH. Compared with the climatological normal, the 5880 gpm isoline is southward and the west ridge point is westward in July 2020, indicating that the WPSH in July 2020 was southward and stronger. The strong WPSH not only inhibited the development of typhoon over the WNP in July 2020, but also made it difficult for the formation of the disturbance of East dispute on its south side.

5.3 SCSMT anomalies

The number of typhoons is limited by the number of tropical disturbances to some extent (Chen and Ding 1979; Zhu et al. 2007). The SCSMT, which is the main source of tropical disturbances over the WNP, has significant differences in location and intensity in different phases of IPO. Figure 9e illustrates the monthly mean horizontal wind field at the 850-hPa level in July 2020, indicating that the intensity of the SCSMT is very weak and the trough line is located west of 120°E, which may be caused by the strong WPSH in the negative phase of IPO in July 2020 (Zhang and Zhang 2011; Qi 2021). The weak SCSMT is unfavorable for the convergence and uplift of airflow. In addition, the low-level vorticity over the WNP in July 2020 is a negative anomaly, which increases the scale of the response and reduces the conversion of latent heat release to rotational motion, thus making it more difficult for the formation of the initial disturbance.

In general, the negative IPO in July 2020 affected large-scale circulation anomalies over the WNP, which reduced the latent heat of condensation released by cumulus convection in the region, strengthened the WPSH, and weakened the SCSMT, hindering the generation of tropical disturbances and typhoons.

5.4 GPI perspective

The aforementioned above discuss three main pathways that IPO affects typhoons in July 2020. Among them, the relative humidity, which represents the convective intensity of cumulus to some extent, is an important factor of GPI. Besides, factors such as vorticity and vertical wind shear are affected by IPO also play a role in typhoon activity. To further verify our results, GPI anomaly is used to characterize the strong inhibition of circulation factors anomalies caused by IPO on the generation of typhoon in July 2020. Figure 12a shows the GPI anomaly over the WNP in July 2020. It reveals that the GPI over the WNP is

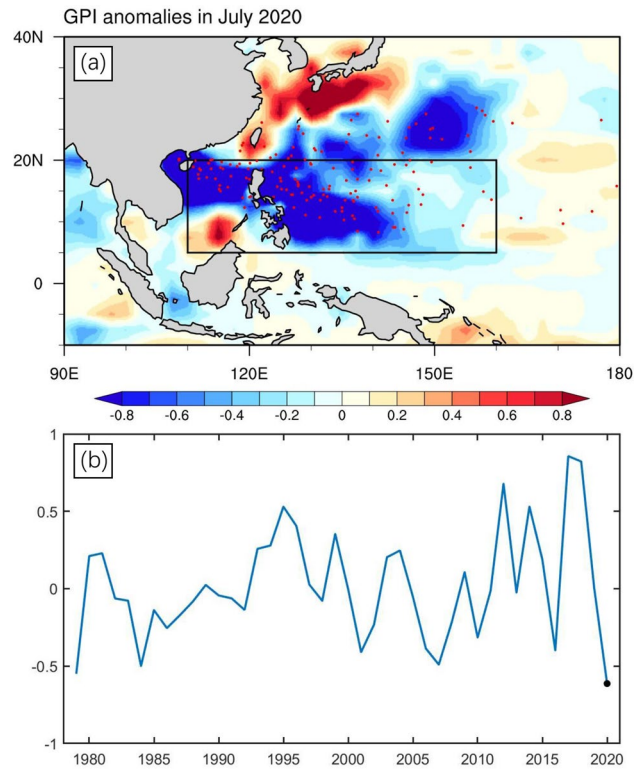
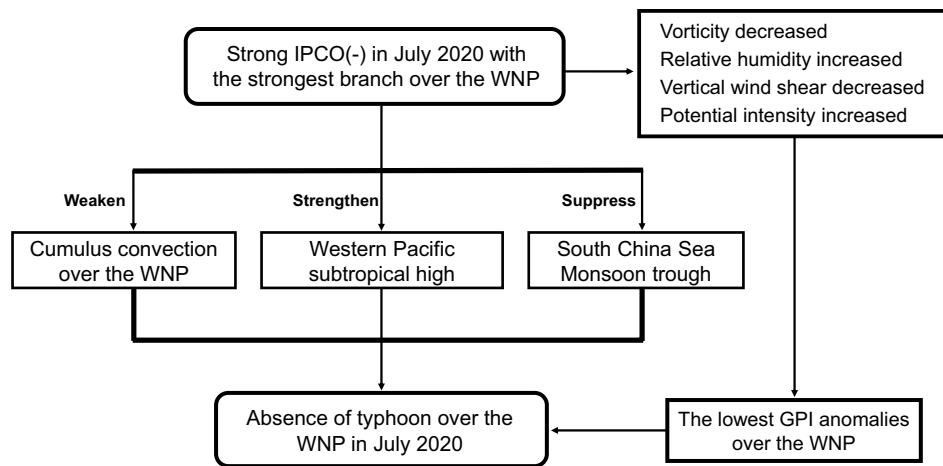


Fig. 12 **a** Anomalies of the GPI in July 2020. The red dots represent the generation location of typhoon from 1979 to July 2020. The black rectangle indicates the same as in Fig. 6. **b** Time series of areal-average GPI anomalies over the WNP (10°N – 25°N , 110°E – 160°E) in July. Dot indicates that the variable in that year had the minimum value over the study period

mostly negative, and the area of the negative GPI anomaly covers most of the generation positions of typhoons over the years, consistent with previous large-scale circulation. As a comprehensive index, the GPI shows that when the strong negative phase of the intraseasonal IPO occurs in July 2020, the anomalies of large-scale atmospheric circulation have an inhibitory effect on typhoon genesis.

We further areal-averaged GPI over the WNP. Figure 12b shows that the GPI anomalies over the WNP in July 2020 were the lowest on record, indicating that the intraseasonal IPO negative phase had the strongest inhibitory effect on typhoon genesis over the WNP by affecting large-scale atmospheric circulation. Previous studies have also shown that relative humidity and vorticity play a leading role in TC genesis compared with the other two factors (Camargo et al. 2009; Wang et al. 2018). Figure 11 shows that the relative humidity and vorticity over the WNP were negative anomalies in July 2020, and the relative humidity was the historical minimum, indicating that the intraseasonal IPO may inhibit the generation of typhoons by affecting the relative humidity.

Fig. 13 The schematic diagram showing the inhibition of the intraseasonal IPCO on typhoon generation in July 2020



6 Conclusion and discussion

In this paper, the inhibitory effect of the intraseasonal IPCO on typhoon genesis in the “absence of typhoons” over the WNP in July 2020 is discussed. The high SST and small vertical wind shear over the WNP in July 2020 are conducive to typhoon genesis, indicating that it is difficult to explain the absence of typhoons from the conditions necessary for typhoon genesis. In contrast, the intraseasonal IPCO plays an important role in modulating the generation of typhoons during the boreal extended summer over the WNP (Wang et al. 2018). This unprecedented absence of typhoon is consistent with IPCO’s unique suppression of convection and the resulting large-scale circulation over the WNP. The influence of atmospheric circulation anomalies caused by IPCO on typhoons, represented by GPI, was the lowest ever recorded. In July 2020, the intraseasonal IPCO turned negative, associated with a strong inhibition on convection over its WNP, leading to large-scale circulation differences and difficulty in generating typhoons.

Three possible ways that affect IPCO typhoon genesis are also presented. Figure 13 shows that the descending movement of the troposphere and low-level divergence were strengthened over the WNP in July 2020, weakening the upward lifting of low-level tropical disturbances and transport of water vapor and inhibiting the development of cumulus convection. Thus, the decrease in the release of latent heat of tropospheric condensation was not conducive to the formation of a typhoon warm-core structure and the development of a cyclone circulation with the increase in height. Due to the inhibition of cumulus convection, tropospheric heating increases by surface long-wave radiation and nonadiabatic heating along with a decrease in altitude, which makes the subtropical high southerly and stronger. This system inhibits the formation and development of typhoons. In addition, when the intraseasonal

IPCO was in its negative phase, the following happened, namely: (a) significant weakening of SCSMT intensity; (b) increase in Rossby deformation radius by increase in the negative vorticity anomaly; (c) increase in the response scale; and (d) reduction in the efficiency of latent heat release into rotational motion. These are not conducive to the generation and development of tropical disturbances. On further employing GPI to examine the influence of large-scale circulation anomalies caused by typhoon genesis, the lowest on record was for July 2020, indicating the strongest suppression of typhoons in history. In general, the negative phase of the intraseasonal IPCO may be one of the main reasons for the extreme large-scale circulation anomalies, leading to the absence of typhoons over the WNP in July 2020.

This study provides an understanding of the absence of typhoons in July 2020 and the benefits of operational climate predictions of typhoon activity. The generation of typhoon is modulated by many factors. Although this study implies that intraseasonal IPCO had an unprecedented inhibitory effect on typhoon in July 2020, various other factors may also play a role in absence of typhoons, which needs further study. For example, Wang et al. (2021) found that the extremely warm Indian Ocean SST may play an important role in the generation of abnormal anticyclones over the WNP and further leads to circulation anomalies and the absence of typhoons. Qi (2021) thought the intensity of the WPSH over the WNP was abnormally strong, the cross-equatorial airflow is weak, making it difficult to form the SCSMT where the typhoon is born, which will significantly affect the frequency of typhoon generation. Besides, the weak El Niño event in winter of 2019/20 may have a limited inhibitory effect on typhoon activity over the WNP in July 2020.

Acknowledgements We thank all the data providers. This work is supported by the National Natural Science Foundation of China (NSFC) Project (41790474), Shandong Natural Science Foundation Project (ZR2019ZD12), and Fundamental Research Funds for the Central

Universities (201962009). We are grateful to Center for High Performance Computing and System Simulation, Pilot National Laboratory for Marine Science and Technology (Qingdao) for providing computing resource.

Author contributions FL and JL contributed to the study conception and design. Material preparation, data collection and analysis were performed by FL. JL and HW analyzed and interpreted the physical mechanism of IPCO's influence on typhoon formation. FL and YD analyzed the influence of IPCO on GPI. The first draft of the manuscript was written by FL, and all authors commented on previous versions of the manuscript. All authors read and approved the final manuscript.

Funding This work is supported by the National Natural Science Foundation of China (NSFC) Project (41790474), Shandong Natural Science Foundation Project (ZR2019ZD12), and Fundamental Research Funds for the Central Universities (201962009).

Data availability The NCEP–NCAR reanalysis data and interpolated OLR data were obtained from <https://psl.noaa.gov/data/gridded/data.ncep.reanalysis.html>. The best-track data for typhoon activity over the WNP by RSMC of JMA were obtained from <http://www.jma.go.jp/jma/jma-eng/jma-center/rsmc-hppub-eg/trackarchives.html>.

Declarations

Conflict of interest I declare that the authors have no competing interests as defined by Springer, or other interests that might be perceived to influence the results and discussion reported in this paper.

Open Access This article is licensed under a Creative Commons Attribution 4.0 International License, which permits use, sharing, adaptation, distribution and reproduction in any medium or format, as long as you give appropriate credit to the original author(s) and the source, provide a link to the Creative Commons licence, and indicate if changes were made. The images or other third party material in this article are included in the article's Creative Commons licence, unless indicated otherwise in a credit line to the material. If material is not included in the article's Creative Commons licence and your intended use is not permitted by statutory regulation or exceeds the permitted use, you will need to obtain permission directly from the copyright holder. To view a copy of this licence, visit <http://creativecommons.org/licenses/by/4.0/>.

References

Anthes RA (1982) Tropical Cyclones: their evolution, structure, and effects. Meteor Monogr, vol 41. American Meteorological Society, p 208

Bister M, Emanuel KA (1998) Dissipative heating and hurricane intensity. *Meteor Atm Phys* 52:233–240

Bessafi M, Wheeler MC (2006) Modulation of south Indian Ocean tropical cyclones by the Madden–Julian oscillation and convectively coupled equatorial waves. *Mon Weather Rev* 134:638–656. <https://doi.org/10.1175/MWR3087.1>

Camargo SJ, Emanuel KA, Sobel AH (2007) Use of a genesis potential index to diagnose ENSO effects on tropical cyclone genesis. *J Clim* 20:4819–4834. <https://doi.org/10.1175/JCLI4282.1>

Camargo SJ, Wheeler MC, Sobel AH (2009) Diagnosis of the MJO modulation of tropical cyclogenesis using an empirical index. *J Atmos Sci* 66:3061–3074. <https://doi.org/10.1175/2009JAS3101.1>

Chen LS, Ding YH (1979) Introduction to typhoons over the Western Pacific (in Chinese). Science Press, Beijing, p 1091

Done J, Hu AX, Farmaer EC, Yin J, Bates S, Frappier AB, Halkides DJ, Kilbourne KH, Sriver R, Woodruff J (2009) The thermohaline circulation and tropical cyclones in past, present, and future climates. *Bull Amer Meteor Soc* 90:1015

Elsberry RL, Tsai HC (2016) Opportunities and challenges in the dynamical and predictability studies of tropical cyclone phases. In: Li JP (ed) Special Publications of the International Union of Geodesy and Geophysics Series, vol 2. Cambridge University Press, pp 133–140

Emmanuel KA (1995) Sensitivity of tropical cyclones to surface exchange coefficients and a revised steady-state model incorporating eye dynamics. *American Meteorological Society* 52(22): 3969–3976. [https://doi.org/10.1175/1520-0469\(1995\)052%3C3969:SOTCTS%3E2.0.CO;2](https://doi.org/10.1175/1520-0469(1995)052%3C3969:SOTCTS%3E2.0.CO;2)

Emanuel K (2001) Contribution of tropical cyclones to meridional heat transport by the oceans. *J Geophys Res* 106:14771–14781

Emmanuel KA, Nolan DS (2004) Tropical cyclone activity and global climate. 26th Conf on Hurricanes and Tropical Meteorology, Miami, FL, Amer Meteor Soc 10A.2

Goldenberg SB, Shapiro LJ (1996) Physical mechanisms for the association of El Niño and West African rainfall with Atlantic major hurricane activity. *J Clim* 9:1169–1187. [https://doi.org/10.1175/1520-0442\(1996\)009%3C1169:PMFTAO%3e2.0.CO;2](https://doi.org/10.1175/1520-0442(1996)009%3C1169:PMFTAO%3e2.0.CO;2)

Gray WM (1968) Global view of the origin of tropical disturbances and storms. *Mon Weather Rev* 96(10):669–700

Gray WM (1979) Hurricanes: their formation, structure and likely role in the tropical circulation. In: Shaw DB (ed) Meteorology over the tropical oceans. Royal Meteorological Society, pp 155–218

Hack JJ, Schubert WH (1986) Nonlinear response of atmospheric vortices to heating by organized cumulus convection. *J Atmos Sci* 43:1559–1573. [https://doi.org/10.1175/1520-0469\(1986\)043,1559:NROAVT.2.0.CO;2](https://doi.org/10.1175/1520-0469(1986)043,1559:NROAVT.2.0.CO;2)

Ho CH, Baik JJ, Kim JH, Gong DY, Sui CH (2004) Interdecadal changes in summertime typhoon tracks. *J Clim* 17:1767–1776. [https://doi.org/10.1175/1520-0442\(2004\)017,1767:ICISTT.2.0.CO;2](https://doi.org/10.1175/1520-0442(2004)017,1767:ICISTT.2.0.CO;2)

Holland GJ (1987) Mature structure and structure change. In: Elsberry RL et al (eds) A global view of tropical cyclones. Office of Naval Research, pp 13–52

Jiang X, Zhao M, Waliser DE (2012) Modulation of tropical cyclones over the eastern Pacific by the intraseasonal variability simulated in an AGCM. *J Clim* 25:6524–6538. <https://doi.org/10.1175/JCLI-D-11-00531.1>

Kalnay E et al (1996) The NCEP/NCAR 40-year reanalysis project. *Bull Amer Meteor Soc* 77:437–471. [https://doi.org/10.1175/1520-0477\(1996\)077,0437:TNYRP.2.0.CO;2](https://doi.org/10.1175/1520-0477(1996)077,0437:TNYRP.2.0.CO;2)

Kepert JD (2010) Tropical cyclone structure and dynamics. In: Chan JCL, Kepert JD (eds) Global perspectives on tropical cyclones: from science to mitigation, world scientific series on Asia-Pacific weather and climate, vol 4. World Scientific, pp 3–54

Lau KM, Chan PH (1985) Aspects of the 40–50 day oscillation during the northern winter as inferred from outgoing longwave radiation. *Mon Weather Rev* 113:1889–1909. [https://doi.org/10.1175/1520-0493\(1985\)113%3C1889:AOTDOD%3E2.0.CO;2](https://doi.org/10.1175/1520-0493(1985)113%3C1889:AOTDOD%3E2.0.CO;2)

Lau KM, Chan PH (1986) Aspects of the 40–50-day oscillation during the northern summer as inferred from outgoing longwave radiation. *Mon Weather Rev* 114:1354–1367. [https://doi.org/10.1175/1520-0493\(1986\)114,1354:AOTDOD.2.0.CO;2](https://doi.org/10.1175/1520-0493(1986)114,1354:AOTDOD.2.0.CO;2)

Lee JY, Wang B, Wheeler MC, Fu X, Waliser DE, Kang IS (2012) Real-time multivariate indices for the boreal summer intraseasonal oscillation over the Asian summer monsoon region. *Clim Dyn* 40:493–509. <https://doi.org/10.1007/s00382-012-1544-4>

Li JP, Wu GX, Hu DX (2011) Ocean–atmosphere interaction over the joining area of Asia and Indian-Pacific Ocean and its impact on the short-term climate variation in China (in Chinese). China Meteorological Press, p 516

Li CY, Pan J, Tian H, Yang H (2012a) Typhoon activity over the western North Pacific and atmospheric intraseasonal oscillation (in Chinese). *Meteor Mon* 38:1–16

Li Y, Li JP, Feng J (2012b) A teleconnection between the reduction of rainfall in southwest western Australia and north China. *J Clim* 25:8444–8461. <https://doi.org/10.1175/JCLI-D-11-00613.1>

Li JP, Sun C, Jin FF (2013a) NAO implicated as a predictor of Northern Hemisphere mean temperature multidecadal variability. *Geophys Res Lett* 40:5497–5502

Li YJ, Li JP, Feng J (2013b) Boreal summer convection oscillation over the Indo-western Pacific and its relationship with the East Asian summer monsoon. *Atmos Sci Lett* 14:66–71. <https://doi.org/10.1002/asl2.418>

Li JP, Swinbank R, Grotjahn R, Volkert H (2016a) Dynamics and predictability of large-scale, high-impact weather and climate phases. *Special Publications of the International Union of Geodesy and Geophysics Series*, vol 2. Cambridge University Press, p 370

Li JP, Wang QY, Li YJ, Zhang JW (2016b) Review and perspective on the climatological research of tropical cyclones in terms of energetics (in Chinese). *J Beijing Norm Univ Nat Sci* 52:705–713

Liebmann B, Smith CA (1996) Description of a complete (interpolated) outgoing longwave radiation dataset. *Bull Amer Meteor Soc* 77:1275–1277

Lu RY (2001) Interannual variability of the summertime North Pacific subtropical high and its relation to atmospheric convection over the warm pool. *J Meteor Soc Japan* 79:771–783. <https://doi.org/10.2151/jmsj.79.771>

Niu HY, Liu M, Lu M (2011) Study on loss assessment of typhoon disaster in coastal areas of China (in Chinese). *J Catastr* 26:61

Palmén E (1948) On the formation and structure of tropical cyclones. *Geophysica* 3:26–38

Pandey RS, Liou YA (2020) Decadal behaviors of tropical storm tracks in the North West Pacific Ocean. *Atmos Res* 261:105644. <https://doi.org/10.1016/j.atmosres.2020.105143>

Pandey RS, Liou YA (2022) Typhoon strength rising in the past four decades. *Weather Clim Extremes* 36:100446. <https://doi.org/10.1016/j.wace.2022.100446>

Pandey RS, Liou YA, Liu JC (2021) Season-dependent variability and influential environmental factors of super-typhoons in the Northwest Pacific basin during 2013–2017. *Weather Clim Extremes* 31:100307. <https://doi.org/10.1016/j.wace.2022.100446>

Pyper BJ, Peterman RM (1998) Comparison of methods to account for autocorrelation in correlation analyses of fish data. *Can J Fish Aquat Sci* 55:2127–2140. <https://doi.org/10.1139/f98-104>

Qi X (2021) Research on the “No-Typhoon July” in 2020 and typhoon frequency variations in July in recent 70 years. *J Geosci Environ Protect* 9:75–83. <https://doi.org/10.4236/gep.2021.91006>

Riehl H (1948) On the formation of typhoons. *J Meteorol* 5:247–264

Ritchie EA, Holland GJ (1999) Large-scale patterns associated with tropical cyclogenesis in the western Pacific. *Mon Weather Rev* 127:2027–2043

Sun C, Li JP, Feng J, Xie F (2015) A decadal-scale teleconnection between the North Atlantic Oscillation and subtropical eastern Australian rainfall. *J Clim* 28:1074–1092. <https://doi.org/10.1175/JCLI-D-14-00372.1>

Wang B, Moon JY (2017) An anomalous genesis potential index for MJO modulation of tropical cyclones. *J Clim* 30:4021–4035. <https://doi.org/10.1175/JCLI-D-16-0749.1>

Wang C, Wu K, Wu LG, Zhao HK, Cao J (2021) What caused the unprecedented absence of western North Pacific tropical cyclones in July 2020? *Geophys Res Lett*. <https://doi.org/10.1029/2020GL092282>

Wang GH, Su JL, Ding YH, Chen DK (2007) Tropical cyclone genesis over the south China sea. *J Mar Syst* 68:318–326

Wang QY, Li JP, Li YJ, Zhang JY (2018) Modulation of tropical cyclogenesis location and frequency over the Indo-western North Pacific by the intra-seasonal Indo-western Pacific convection oscillation during the boreal extended summer. *J Clim* 31:1435–1450. <https://doi.org/10.1175/JCLI-D-17-0085.1>

Wang QY, Li JP, Li YJ, Xue JQ, Zhao S, Xu YD, Wang YH, Zhang YZ, Dong D, Zhang JW (2019) Modulation of tropical cyclogenesis tracks over the Indo-western North Pacific by the intra-seasonal Indo-western Pacific convection oscillation during the boreal extended summer. *J Clim* 52:913–927. <https://doi.org/10.1007/s00382-018-4264-6>

Xie F, Li JP, Tian WS, Zhang JK, Sun C (2014) The relative impacts of El Niño Modoki, canonical El Niño, and QBO on tropical ozone changes since the 1980s. *Environ Res Lett* 9:064020. <https://doi.org/10.1088/1748-9326/9/6/064020>

Zhang C, Zhang QH (2011) Spatial temporal characteristics of tropical disturbances over the Northwestern Pacific during 2000–2008. *Acta Scientiarum Naturalium Universitatis Pekinensis* 47(2):278–286

Zhang JW, Li JP, Li YJ (2015) Intraseasonal characteristics of the Indo-west Pacific convection oscillation (in Chinese). *Chin J Atmos Sci* 39:221–234

Zhao HK, Jiang X, Wu L (2015a) Modulation of northwest Pacific tropical cyclone genesis by the intraseasonal variability. *J Meteor Soc Japan* 93:81–97. <https://doi.org/10.2151/jmsj.2015-006>

Zhao HK, Yoshida R, Raga GB (2015b) Impact of the Madden–Julian oscillation on western North Pacific tropical cyclogenesis associated with large-scale patterns. *J Meteor Soc Japan* 54:1413–1429. <https://doi.org/10.1175/JAMC-D-14-0254.1>

Zheng HY, Wu L, Wen ZP (2013) Characteristics of typhoon frequency in the western North Pacific and its relation to the air-sea fluxes (in Chinese). *Acta Oceanol Sin* 35:47–55

Zheng JY, Li YJ, Li JP, Xue JQ, Guo YP, Liu T, Wang QY (2017) The relationship between Indo-Pacific convection oscillation and summer surface air temperature in Southern Asia. *Sola* 13:199–204. <https://doi.org/10.2151/sola.2017-036>

Zhu BZ, Wang B (1993) The 30–60-day convection seesaw between the tropical Indian and western Pacific Oceans. *J Atmos Sci* 50:184–199. [https://doi.org/10.1175/15200469\(1993\)050,0184:TDCSBT.2.0.CO;2](https://doi.org/10.1175/15200469(1993)050,0184:TDCSBT.2.0.CO;2)

Zhu QG, Lin JR, Shou SW (2007) *Synoptic principles and methods* (in Chinese). Meteorological Press, Beijing, pp 508–550

Publisher's Note Springer Nature remains neutral with regard to jurisdictional claims in published maps and institutional affiliations.